

Adaptive Control Strategy for Improving Small-signal Stability of Multiple Grid-connected Converter Systems

Zhenxiang Liu, Yanbo Chen, *Senior Member, IEEE*, Jiahao Ma, and Zhi Zhang, *Member, IEEE*

Abstract—The high penetration of renewable energy sources interfaced through power electronic converters often leads to small-signal stability issues. Therefore, it is critical to quantify the impact of control parameters in multiple grid-connected converters on the small-signal stability of power system. To this end, this paper derives the small-signal stability criterion and provides the quantitative analysis of parameter sensitivity for multiple grid-connected converter systems (MGCCSs) based on extended Gershgorin theorem, thereby clarifying the influence of control parameters on the small-signal stability and providing the foundation for adaptive control. Crucially, leveraging this sensitivity analysis, we propose an adaptive control strategy involving targeted parameter adjustment for the identified weak links to ensure that the system operates with a specified stability margin. Both theoretical analysis and simulation prove the effectiveness of the proposed adaptive control strategy in the improving the small-signal stability of MGCCSs. Importantly, the proposed adaptive control strategy also demonstrates the significant potential for online application to adaptively compensate the small-signal stability margin in real time.

Index Terms—Grid-connected converter system, adaptive control, parameter sensitivity, small-signal stability.

I. INTRODUCTION

UNDER the penetration of a high proportion of power electronic equipment, the interaction between the converter group and power grid may lead to the oscillation problem in the system. This problem has become an important factor that restricts the consumption of renewable energy and seriously threatens the stable operation of power system [1]-[3]. Therefore, the modeling and stability analysis meth-

ods of such systems have attracted the extensive attention of academic and industrial communities.

At present, the oscillation problem of multiple grid-connected converter systems (MGCCSs) can be analyzed from the perspective of small-signal stability [4]. The eigenvalue analysis method based on the state-space model studies the system small-signal stability by establishing the overall system state-space model. But the order of the system state-space model increases with the increase of system scale, which is not conducive to large-scale systems. Therefore, this method is not conducive to providing guidance information such as small-signal stability margins for MGCCSs [5]-[7].

The conciseness of impedance model has driven significant interests in its use for stability analysis of large-scale systems [8]-[10]. Some corresponding frequency-domain stability criteria, such as the Nyquist trajectory criterion [11], modal analysis [12], and extended Gershgorin theorem [13], are widely applied to MGCCSs. Modal analysis solves poles of the admittance matrix, while other studies emphasize the role of matrix determinant zeros or use the generalized Nyquist criterion (GNC) [14]-[16]. However, these methods often face dimensionality challenges in multi-input multi-output (MIMO) systems. Moreover, the time-varying stability boundaries influenced by renewable energy randomness necessitate fast solutions. Although the eigenvalue estimation based on Gershgorin theorem and G-sum norm offers computational speed, its high conservativeness remains a key limitation [17]. When adopting highly conservative small-signal stability criteria for analysis, it can lead to problems such as unclear stability boundaries and imprecise parameter sensitivity calculations, making it difficult to apply in engineering practice. In our preliminary research, we establish a small-signal stability criterion for MGCCSs based on the extended Gershgorin theorem [18]. This significantly reduces the conservativeness inherent in traditional methods and also serves as the foundation for the research presented in [19]. The significance of these works lies in reducing the conservativeness of small-signal stability criteria, making it more conducive to clarifying the impact of control parameters on system small-signal stability.

At present, most studies focus on the influencing factors of the small-signal stability of grid-connected converter systems by changing the control parameters to observe the trend of system stability changes. This indirect analysis meth-

Manuscript received: January 10, 2025; revised: May 11, 2025; accepted: July 17, 2025. Date of CrossCheck: July 17, 2025. Date of online publication: August 29, 2025.

This work was supported by the National Natural Science Foundation of China (No. U24B2083) and the Fundamental Research Funds for the Central Universities (No. 2025JC001).

This article is distributed under the terms of the Creative Commons Attribution 4.0 International License (<http://creativecommons.org/licenses/by/4.0/>).

Z. Liu, Y. Chen (corresponding author), J. Ma, and Z. Zhang are with the School of Electrical and Electronic Engineering, North China Electric Power University, Beijing 102206, China, and Y. Chen is also with State Key Laboratory of Alternate Electrical Power System with Renewable Energy Sources, North China Electric Power University, Beijing 102206, China, Qinghai Institute of Technology, Xining 810016, China, and Jiangxi University of Water Resources and Electric Power, Nanchang 330099, China (e-mail: 11z2x3@qq.com; yanbochen2008@sina.com; AA1091312147@163.com; 957558366@qq.com).

DOI: 10.35833/MPCE.2025.000029



od cannot intuitively and quantitatively analyze the influence of control parameters on the small-signal stability [20], [21]. From the view of control parameter design, most studies focus on the interactions between control parameters and converter behaviors [22]-[24]. Reference [22] elaborates on the strong interaction between the control loops inside the converter under weak grid conditions, and uses the sensitivity function to show how the stability margin varies with the changing control parameters. References [23] and [24] discuss the establishment of impedance model for voltage source converter (VSC) including phase-locked loop (PLL) dynamics, and use the developed impedance model to analyze the effect of different PLL bandwidths on the converter stability. All the above methods focus on single grid-connected converter system, and there is no report on analyzing the influence of control parameters on the overall stability of MGCCSs. Reference [25] points out that in MGCCSs, the optimal strategy for determining the control parameters according to the system small-signal stability margin is not yet clear. It is particularly important to clarify the influence of control parameters on the system small-signal stability margin and to give the criterion.

This paper implements an adaptive control strategy for MGCCSs, which need to efficiently select the control parameters based on the parameter sensitivity analysis. The mainstream commercial optimization solutions are often unsuitable, primarily due to the nonlinear components and locally non-analytical representations in the objective function of MGCCSs, which are inherent characteristics of complex power electronic systems. To enable the practical and effective adaptive control, algorithms robust to these complexities are essential. Reference [26] highlights the low sensitivity of particle swarm optimization (PSO) algorithm to model accuracy, thus making it well-suited for power electronic applications, where the precise modeling can be difficult. References [27] and [28] demonstrate that algorithms such as simulated annealing (SA), genetic algorithm (GA), and differential evolution algorithm (DEA) exhibit strong convergence properties when optimizing control parameters. Therefore, to realize the adaptive control strategy, this paper employs SA, GA, DEA, and PSO to solve the optimization model for control parameters. A comparative analysis of these optimization algorithms is conducted, specifically evaluating their applicability to the adaptive control, convergence behavior, and computational speed.

The main contributions of this paper are summarized as follows.

1) This paper provides a small-signal stability criterion based on the extended Gershgorin theorem. Furthermore, an optimization model for the control parameters of MGCCSs is established based on this criterion.

2) In order to better respond to the high-dimensional, nonlinear, and nonconvex characteristics of this optimization model, the quantitative criteria for parameter sensitivity of MGCCSs are derived in this paper. Based on this, adjusting the parameters of weak control link not only ensures a certain stability margin of the system, but also greatly reduces the computational dimension and iteration number of the op-

timization algorithm.

3) There are few reports on how to self-adaptively adjust the control parameters considering the time-varying characteristics of the small-signal stability margin brought by the randomness and volatility of renewable energy. Its core lies in the computational efficiency of the online stability margin evaluation. Therefore, combining the extended Gershgorin theorem, which offers lower computational complexity, with sensitivity-based control parameter selection methods can significantly reduce the solution time of optimization algorithms.

The rest of this paper is arranged as follows. Section II presents the frequency-domain modeling for MGCCSs. The small-signal stability criterion and quantitative analysis of parameter sensitivity based on extended Gershgorin theorem are given in Section III. Section IV investigates the proposed adaptive control strategy through theoretical analysis and simulation experiments. Finally, the conclusions are made in Section V.

II. FREQUENCY-DOMAIN MODELING FOR MGCCSs

The topology of MGCCSs for the analysis of this paper is shown in Fig.1. There are n aggregated converter groups connected to the grid through passive transmission network, where the converter group corresponding to the k^{th} feed-in node is denoted as C_k . In order to facilitate the establishment of a negative feedback model in the frequency domain, the whole system is divided into active and passive subsystems.

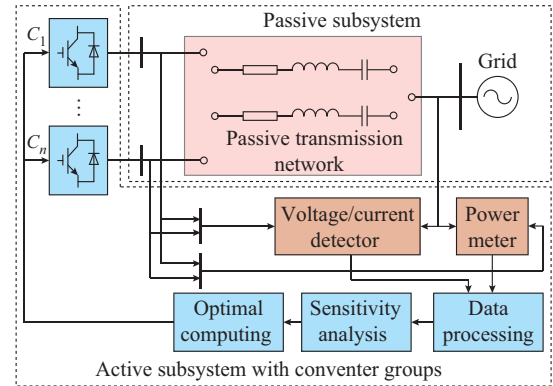


Fig. 1. Topology of MGCCSs.

The grid-connected converters are mostly controlled in the dq coordinates. The sampling point of the PLL takes the feedback signal of the local point of common coupling (PCC). The modeling method of local dq coordinates does not take into account the voltage deviation between multiple nodes. Therefore, it is necessary to introduce a linear transformation matrix T_k to convert the local dq coordinates to the global coordinates. Define θ_k as the phase angle difference for the voltage sampling of the k^{th} converter group. The admittance model of each converter group is expressed as:

$$T_k^{-1} \mathbf{i}_{sk} = \mathbf{i}_k^* - Y_{sk} T_k^{-1} \mathbf{u}_{sk} \quad (1)$$

where $\mathbf{i}_{sk} = [i_{sdk}, i_{sqk}]^T$ and $\mathbf{u}_{sk} = [u_{sdk}, u_{sqk}]^T$ are the current and voltage vectors of active nodes in the local dq coordinate, respectively; Y_{sk} is the output admittance of active node port; \mathbf{i}_k^* is the small disturbance of the system; and $T_k =$

$\begin{bmatrix} \cos \theta_k & \sin \theta_k \\ -\sin \theta_k & \cos \theta_k \end{bmatrix}$. The detailed derivation process of Y_{sk} can be found in Supplementary Material A. The matrix-form expression considering multiple converter groups is given as:

$$\mathbf{i} = \mathbf{T}\mathbf{i}^* - \mathbf{T}\mathbf{Y}_s\mathbf{T}^{-1}\mathbf{u} \quad (2)$$

$$\mathbf{u} = \mathbf{Z}_L\mathbf{i} \quad (3)$$

where $\mathbf{i} = [i_1, i_2, \dots, i_n]^T$ and $\mathbf{u} = [u_1, u_2, \dots, u_n]^T$ are the port current and voltage matrices of n converter groups, respectively; $\mathbf{i}^* = \text{diag}(i_1^*, i_2^*, \dots, i_n^*)$; $\mathbf{T} = \text{diag}(T_1, T_2, \dots, T_n)$; $\mathbf{Y}_s = \text{diag}(Y_{s1}, Y_{s2}, \dots, Y_{sn})$; and \mathbf{Z}_L is the impedance network matrix of passive subsystem. By combining (2) and (3), we have:

$$\mathbf{i} = (\mathbf{I}_{2n} + \mathbf{T}\mathbf{Y}_s\mathbf{T}^{-1}\mathbf{Z}_L)^{-1}\mathbf{T}\mathbf{i}^* \quad (4)$$

where \mathbf{I}_{2n} is an identity matrix with dimension of $2n$.

Equation (4) shows a closed-loop negative feedback model. The open-loop transfer function $\mathbf{H} = \mathbf{Z}_L\mathbf{T}\mathbf{Y}_s\mathbf{T}^{-1}$ is defined. Reference [18] points out that the addition, multiplication, and inverse operations are closed for matrices in the form of $\mathbf{F} = \begin{bmatrix} a & -b \\ b & a \end{bmatrix}$. Meanwhile, the matrix for the RLC passive transmission network only involves basic algebraic operations. Obviously, the same conclusion exists for the linear transformation matrix \mathbf{T} . Therefore, the open-loop transfer function of the negative feedback model is obtained from the multiplication commutative law:

$$\mathbf{H} = \mathbf{T}\mathbf{Z}_L\mathbf{Y}_s\mathbf{T}^{-1} \quad (5)$$

The linear transformation guided by the unit orthogonal matrix \mathbf{T} does not change the eigenvalues of original matrix. Therefore, the impedance ratio matrix $\mathbf{L} = [L_{ij}] = \mathbf{Z}_L\mathbf{Y}_s$ can be defined.

III. SMALL-SIGNAL STABILITY ANALYSIS FOR MGCCSS

After obtaining the impedance ratio matrix, the small-signal stability analysis can be conducted using either eigenvalue calculation or estimation methods. The characteristics of different stability analysis methods are summarized in Table I. It is evident that the exact eigenvalue calculation introduces higher computational complexity, which is disadvantageous for the adaptive adjustment of control parameters in MGCCSSs. Therefore, the focus should be placed on eigenvalue estimation. Both the Gershgorin theorem and extended Gershgorin theorem effectively reduce the computational complexity. However, the Gershgorin theorem tends to be overly conservative in its estimation range, which may prevent the system from maintaining a high small-signal stability margin over the entire operational period, as demonstrated in [19]. In light of this, this study opts to construct an optimization model based on the extended Gershgorin theorem, which aims to balance lower computational complexity with improved accuracy in eigenvalue estimation.

TABLE I
CHARACTERISTICS OF DIFFERENT STABILITY ANALYSIS METHODS

Analysis method	Stable condition	Quantitative standard	Calculation method	Conservative	Computation order
Eigenvalue calculation	$\xi > 0$	Damping ratio and oscillation frequency	QR decomposition of higher-order matrices	Necessary and sufficient condition	$O(n^3)$
GNC	$N_+ = N_-$	Phase margin amplitude margin	Repeated QR decomposition	Necessary and sufficient condition	$O(n^3)$
Gershgorin theorem	$g(\omega) > 0$	Oscillation frequency estimation	Elementary calculation	Sufficient condition	$O(n)$
Extended Gershgorin theorem	$f(\omega) > 0$	Oscillation frequency estimation	Elementary calculation	Sufficient and less conservative condition	$O(n^2)$

Note: ξ is the damping ratio; N_+ and N_- are the numbers of circles enclosed in the counterclockwise and clockwise directions, respectively; and $g(\omega)$ and $f(\omega)$ are the stability criteria based on Gershgorin theorem and extended Gershgorin theorem, respectively.

A. Stability Criterion Based on Extended Gershgorin Theorem

According to the extended Gershgorin theorem, the eigenvalues of the $2n$ -order matrix \mathbf{L} are distributed within the union of $2n$ disks centered on its diagonal elements [19]. S_{ri} and S_{cj} are the estimated regions of the row and column Gershgorin circles, whose expressions are given in (6) and (7), respectively. The row (column) radius is the sum of prime modulus values for the non-diagonal element of the corresponding row (column).

$$S_{ri}: \left\{ (x, y) \left| \sqrt{(x - \text{Re}(L_{ii}))^2 + (y - \text{Im}(L_{ii}))^2} \leq \sum_{j=1, j \neq i}^n |L_{ij}| \right. \right\} \quad (6)$$

$$S_{cj}: \left\{ (x, y) \left| \sqrt{(x - \text{Re}(L_{jj}))^2 + (y - \text{Im}(L_{jj}))^2} \leq \sum_{i=1, i \neq j}^n |L_{ij}| \right. \right\} \quad (7)$$

where (x, y) is the estimation area for eigenvalues of matrix \mathbf{L} .

According to the properties of Gershgorin circle, the estimation region M of eigenvalues can be obtained [29], with the following expression:

$$M = \left\{ \left(\bigcup_{i=1}^n S_{ri} \right) \cap \left(\bigcup_{j=1}^n S_{cj} \right) \right\} \quad (8)$$

According to the set distributive property, rewrite the above formula, and replace the intersection region of any two Gershgorin circles with a disk O_{ij} . The criterion obtained by this method is still sufficient. Therefore, the estimation region M of eigenvalues can be reshaped as:

$$M = \left\{ \bigcup_{i=1, j=1}^n O_{ij}, O_{ij} \geq S_{ri} \cap S_{cj} \right\} \quad (9)$$

The width of the forbidden domain is defined as r , and

the geometric meaning of (9) is shown in Fig. 2, which illustrates the eigenvalue estimation via extended Gershgorin theorem. In order to quantify the small-signal stability of system, it is necessary to know several specific distances, which are R_{aij} , R_{bij} , R_{cij} , R_{Tc} , and R_{Tr} , as labeled in Fig. 2.

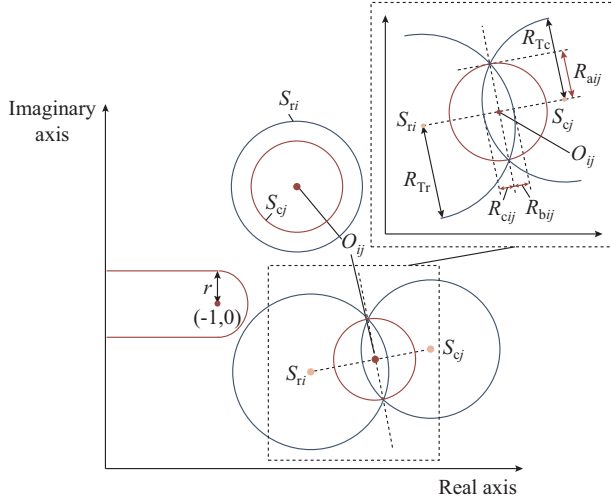


Fig. 2. Geometric meaning of (9) illustrating eigenvalue estimation via extended Gershgorin theorem.

For the small-signal stability analysis of MGCCSs, the geometric significance of the sufficient criterion based on the extended Gershgorin theorem is shown in Fig. 3. By defining the oscillation band (OB), the stable region, unstable region, and region with instability risk of the system can be intuitively determined.

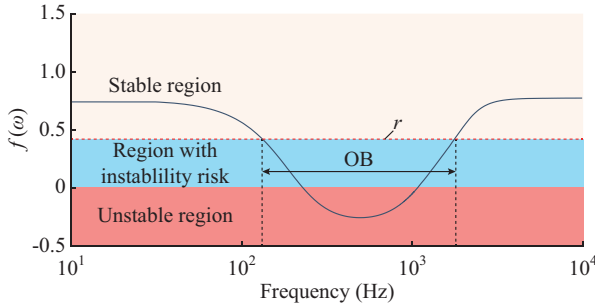


Fig. 3. Geometric significance of sufficient criterion based on extended Gershgorin theorem.

For any frequency ω satisfying $f(\omega) > r$, the corresponding MGCCSs are stable. The algebraic expression for $f(\omega)$ is:

$$f(\omega) = \min \begin{cases} \left| \text{Im}(O_{ij}) \right| - \max(R_{aij}, R_{bij}, R_{cij}) & \text{Re}(O_{ij}) \leq -1 \\ \left| O_{ij} + 1 \right| - \max(R_{aij}, R_{bij}, R_{cij}) & \text{Re}(O_{ij}) > -1 \end{cases} \quad (10)$$

From the perspective of enhancing the overall system stability margin, determining the threshold for low small-signal stability margin or identifying when system parameters require adjustment remains a critical issue. According to [19], the extended Gershgorin theorem has addressed the high conservative problem of eigenvalue estimation algorithms. This only includes elementary operations with low computational

complexity. The size of regions with instability risk is determined by r . Obviously, the larger r is, the more conservative the theorem is to judge the system small-signal stability.

It is important to distinguish between the unstable region ($f(\omega) < 0$) and the region with instability risk ($0 \leq f(\omega) \leq r$) where the system, although potentially stable by the strict criterion, possesses a low stability margin, thus triggering adaptive control actions to prevent potential instability. That is, when the minimum value of $f(\omega)$ ($\min f(\omega)$) is in the region with instability risk, the procedure of adjusting the control parameters will be started.

Unlike fixed controllers, the proposed adaptive control strategy detects the region with instability risk and initiates preemptive parameter adjustments to actively increase the stability margin before the instability occurs. This transforms stability management from passive monitoring into active assurance, significantly enhancing the system resilience and safety.

B. Quantitative Analysis of Parameter Sensitivity

From the definition of the small-signal stability criterion in Section III-A, if the control parameters are taken as independent variables, $f(\omega)$ can be regarded as a multivariate function. Define x as the adjustable control parameter in the system and x_0 as its initial value. The sensitivity function $k(\omega)$ of the system according to the definition of the partial derivative is defined as:

$$k(\omega) = \left. \frac{\partial f(\omega, x_0)}{\partial x} \right|_{x=x_0} \quad (11)$$

It is worth mentioning that in the specific calculation process, there are two methods for solving (11). First, $f(\omega)$ can be fit into a mathematical expression, and then its partial derivative is solved. However, the fitting of function images and the solution of partial derivative will have adverse effects on the calculation speed. Second, it can be solved by using the definition of partial derivative. Considering that the central difference has higher second-order accuracy than the forward and backward differences, the sensitivity function can be expressed as:

$$k(\omega) = \lim_{\Delta x \rightarrow 0} \frac{f(\omega_0, x_0 + \Delta x) - f(\omega_0, x_0 - \Delta x)}{2\Delta x} \quad (12)$$

where ω_0 is the fixed value of frequency sampling point; and Δx is the micro-increment of control parameter.

As shown in Fig. 4, it is assumed that the sensitivity functions of four different control parameters in the system are denoted as $k_1(\omega)$, $k_2(\omega)$, $k_3(\omega)$, and $k_4(\omega)$.

Comparing the curves of $k_1(\omega)$ and $k_2(\omega)$, it can be observed that the influence of the control parameter represented by $k_1(\omega)$ is greater than that represented by $k_2(\omega)$ in the whole frequency band. At the same time, the values of $k_1(\omega)$ and $k_2(\omega)$ are always greater than 0, indicating that the adjustment trends of the two control parameters are consistent with the changing trend of the small-signal stability margin. That is to say, the improvement of system stability can be achieved by increasing the value of these two control parameters. Conversely, for the curves $k_3(\omega)$ and $k_4(\omega)$, the values of the corresponding control parameter should be reduced.

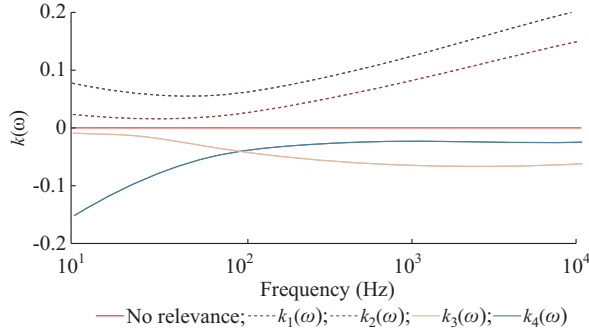


Fig. 4. Curves of sensitivity functions with four different control parameters.

When the obtained curves $k_3(\omega)$ and $k_4(\omega)$ intersect at some points, the influence of the corresponding control parameters on the stability of the system on both sides of that frequency point is completely opposite. While the magnitude of $k(\omega)$ indicates the influence strength of a control parameter, its sign is crucial as it dictates the required adjustment direction to enhance the system stability. Ignoring the sign would hinder the effective improvement of small-signal stability. At the same time, a clear standard is needed to selecting the adjustable control parameters in MGCCSs. Define the set of discrete points of control parameter x in ascending order as $\{x_1, x_2, \dots, x_m\}$, where x_1 and x_m are the lower and upper bounds of adjustable control parameter, respectively. The parameter sensitivity s can be defined as:

$$s = \sum_{e=1}^m k_e(\omega_0) \Delta x \geq |\min f(\omega)| + r \quad (13)$$

where $k_e(\omega_0)$ is the sensitivity function at point x_e .

If a certain adjustable control parameter x satisfies (13), it has the ability to tune the unstable system to a system with certain stability margin.

C. Improvement of Small-signal Stability

In this subsection, we establish an optimization model for MGCCSs, with the objective function being:

$$F = \max(\min f(\omega)) \quad (14)$$

$$pos = R_{1,i}^2 - R_{2,j}^2 + 2R_{1,i}O_L - O_L^2 \quad (15)$$

$$O_L = \sqrt{(\text{Re}(L_{ii}) - \text{Re}(L_{jj}))^2 + (\text{Im}(L_{ii}) - \text{Im}(L_{jj}))^2} \quad (16)$$

$$\begin{cases} R_{1,i} = \sum_{j=1, j \neq i}^{2n} |L_{ij}| \\ R_{2,j} = \sum_{i=1, i \neq j}^{2n} |L_{ij}| \end{cases} \quad (17)$$

where pos is a quantity that describes the positional relationship between two disks.

If $pos \geq 0$, then:

$$\begin{aligned} O_{ij} = & \text{Re}(L_{ii}) + (R_{1,i} - R_{bij}) \cos(arg) - \max(R_{ajj}, R_{bij}, R_{cij}) + \\ & j[\text{Im}(L_{ii}) + (R_{1,i} - R_{bij}) \sin(arg) - \max(R_{ajj}, R_{bij}, R_{cij})] \end{aligned} \quad (18)$$

$$\begin{cases} R_{ajj} = \frac{R_{1,i}^2 - R_{2,j}^2 + 2R_{1,i}O_L - O_L^2}{2O_L} \\ R_{bij} = R_{1,i} + R_{2,j} - O_L - R_{ajj} \\ R_{cij} = \sqrt{R_{1,i}^2 - (R_{1,i} - R_{bij})^2} \end{cases} \quad (19)$$

$$arg = \arctan \frac{\text{Im}(L_{jj}) - \text{Im}(L_{ii})}{\text{Re}(L_{jj}) - \text{Re}(L_{ii})} \quad (20)$$

If $pos < 0$, then:

$$\begin{aligned} O_{ij} = & \text{Re}(L_{ii}) + (R_{bij} - R_{1,i}) \cos(arg) - \max(R_{ajj}, R_{bij}, R_{cij}) + \\ & j[\text{Im}(L_{ii}) + (R_{bij} - R_{1,i}) \sin(arg) - \max(R_{ajj}, R_{bij}, R_{cij})] \end{aligned} \quad (21)$$

$$\begin{cases} R_{ajj} = \frac{R_{2,j}^2 - R_{1,i}^2 + 2R_{2,j}O_L + O_L^2}{2O_L} \\ R_{bij} = R_{1,i} + R_{2,j} - O_L - R_{ajj} \\ R_{cij} = \sqrt{R_{1,i}^2 - (R_{1,i} - R_{bij})^2} \end{cases} \quad (22)$$

The main difficulty in solving this optimization model is the presence of nonlinear components in the objective function and local non-analytical representations. Its mathematical essence is the solving process of nonlinear and nonconvex optimization.

The computational complexity of optimization algorithm for improving the small-signal stability increases with the number of input variables. Based on the parameter sensitivity s , the control parameters can be selected to participate in regulation. In this way, the number of input variables for optimization algorithm can be greatly reduced to ensure high rate of convergence and calculation speed. The flow chart of improving the small-signal stability based on optimization algorithm is shown in Fig. 5.

Firstly, periodically monitor the system status or collect real-time measurement data such as voltage and current of key nodes triggered by events. When the value of $\min f(\omega)$ is located in the region with instability risk or the unstable region, the program for adjusting the control parameters will be started.

The specific process is: first, compare the sensitivity functions $k(\omega)$ of different control parameters. And select control parameters as input variables of optimization algorithm according to (13). When the optimization algorithm finishes iterating, if the proposed adaptive control strategy is used for the planning and design of system small-signal stability, its return value can be called directly. Furthermore, if the proposed adaptive control strategy is used for online compensation of control parameters, the process needs to be executed iteratively. This undoubtedly has extremely high requirements on the calculation speed of optimization algorithm. The time-scales for measuring the randomness and fluctuation characteristics of new energy or changes in system operation mode are usually hours or minutes. Therefore, this method can meet the interference caused by the randomness and fluctuation characteristics of new energy when compensating the system control parameters online.

It is worth mentioning that this paper not only ensures a certain small-signal stability margin of the system by adjusting the control parameters of the weak control link, but also

proposes an objective function based on the extended Gershgorin theorem, which can greatly reduce the computational dimension and iteration number of optimization algorithm.

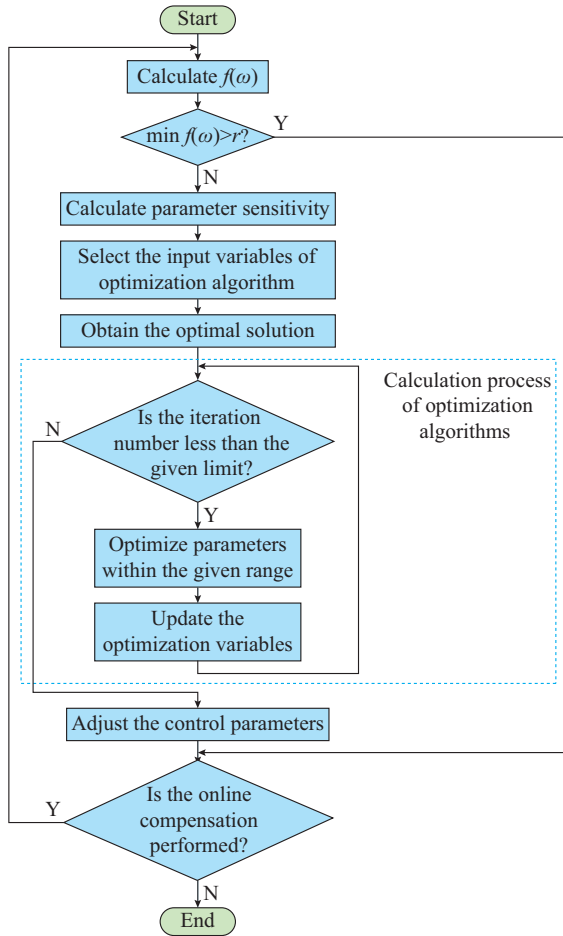


Fig. 5. Flow chart of improving small-signal stability based on optimization algorithms.

IV. SIMULATION RESULTS

As shown in Fig. 6, the MGCCS example consists of 7 active nodes. Table II lists the power fed by active nodes, where Case A represents the initial operating state of the system, Case B represents the state after the system stability has been improved by optimization algorithm, e. g., PSO, and Cases C-F represent the validation groups with different power generation capacities.

By designing multiple power generation capacity configurations, the effectiveness and universality of the proposed adaptive control strategy can be better verified. The passive network parameters and inverter topology used in this paper can be found in [19]. The control parameters of inverter are detailed in Supplementary Material B.

According to the description of r in Section III, it is not difficult to determine the range of r as $0 \leq r < \max f(\omega)$. When $r > \max f(\omega)$, the width of forbidden domain will lose its significance. It is worth noting that different values of r can affect the startup time of optimization algorithm. When $r = 0$, the conservativeness of this criterion is the lowest. This paper only takes the case of $r = 0.05$ in the experiment

as an example. A numerical example illustrates the specific implementation process of the proposed adaptive control strategy. At the same time, this section also discusses that the proposed adaptive control strategy can improve the overall small-signal stability of the system under different grid strengths.

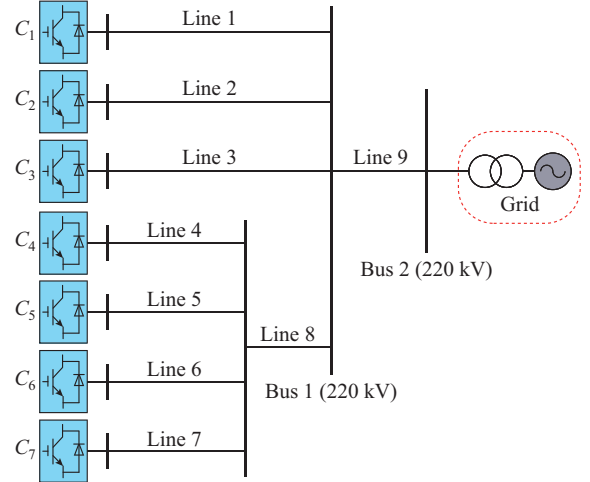


Fig. 6. Topology of MGCCS example.

TABLE II
POWER FED BY ACTIVE NODES

Converter group	Power (GW)				
	Cases A and B	Case C	Case D	Case E	Case F
C_1	0.2	0.2	0.2	0.2	0.3
C_2	0.2	0.2	0.2	0.5	0.3
C_3	0.1	0.2	0.3	0.1	0.2
C_4	0.2	0.1	0.2	0.1	0.1
C_5	0.1	0.2	0.1	0.1	0.1
C_6	0.1	0.2	0.1	0.1	0.1
C_7	0.3	0.1	0.1	0.1	0.1
Total	1.2	1.2	1.2	1.2	1.2

It can be observed from Fig. 7 that the value of $\min f(\omega)$ in Case A is below the straight line ($r = 0.05$). This indicates that Case A has entered the unstable region, thus triggering the adaptive optimization process for control parameters.

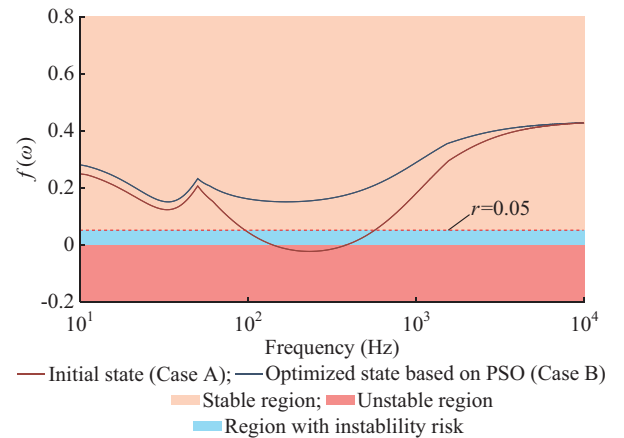


Fig. 7. Curves of $f(\omega)$ in Case A and Case B.

This paper focuses on the sensitivity functions of six control parameters, i.e., proportional coefficient of PLL K_{pll} , integral coefficient of PLL K_{pli} , proportional coefficient of DC-link voltage outer-loop K_{pu} , integral coefficient of DC-link voltage outer-loop K_{iu} , proportional coefficient of current inner-loop K_{pi} , and integral coefficient of current inner-loop

K_{ii} . The sensitivity functions of these six control parameters can be obtained by calculation, the curves of which in Case A are shown in Fig. 8(a)-(f), respectively, where these control parameters of the k^{th} converter group are denoted with subscript k and the horizon axis adopts the logarithmic coordinate. The parameter sensitivities are shown in Fig. 9.

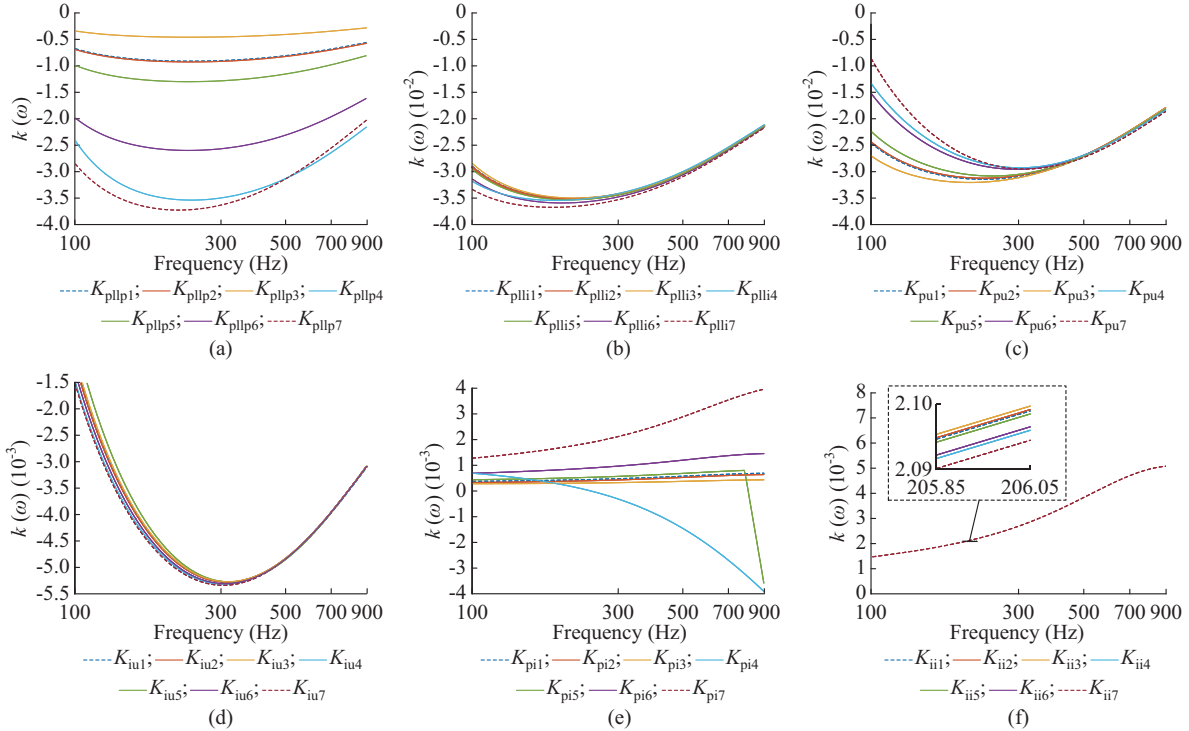


Fig. 8. Sensitivity function curves of six control parameters. (a) Sensitivity function of K_{pll} . (b) Sensitivity function of K_{pli} . (c) Sensitivity function of K_{pu} . (d) Sensitivity function of K_{iu} . (e) Sensitivity function of K_{pi} . (f) Sensitivity function of K_{ii} .

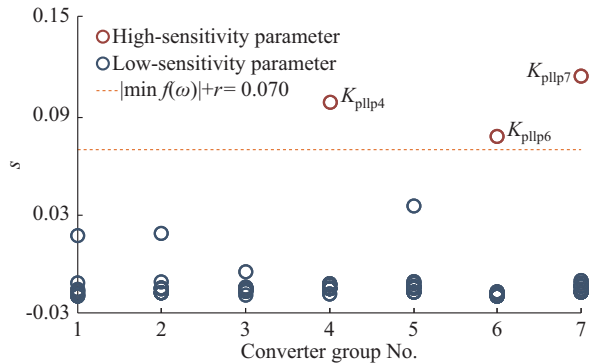


Fig. 9. Diagram of parameter sensitivity.

By observing the sensitivity function $k(\omega)$ and parameter sensitivity s , two conclusions can be drawn. First, the sensitivity of K_{pll} is very high compared with that of other control parameters. In Fig. 9, the sensitivity s for K_{pll4} , K_{pll6} , and K_{pll7} satisfies (13), which can be defined as high-sensitivity parameters and selected to participate in the adjustment. Second, taking Fig. 8(a) as an example, the sensitivity functions $k(\omega)$ of all converter groups are all less than 0, which means the small-signal stability is negatively correlated with K_{pll} .

Next, we will discuss the applicability of the proposed

adaptive control strategy under different power generation capacity configurations. Table III shows the prerequisites for sensitivity analysis of Cases A and C-F. Among them, Case C is consistent with Case A and initially runs in an unstable state. The initial operating state of the other three groups is stable.

TABLE III
PREREQUISITES FOR SENSITIVITY ANALYSIS OF CASES A AND C-F

Case	Initial state	$\min f(\omega)$	$ \min f(\omega) + r$
Case A	Unstable	-0.020	0.070
Case C	Unstable	-0.057	0.107
Case D	Stable	0.159	0.209
Case E	Stable	0.232	0.282
Case F	Stable	0.235	0.285

As shown in Fig. 10, the parameter sensitivity calculation can be used to screen high-sensitivity parameters in different cases. On the one hand, it can reshape the originally unstable MGCCSs. On the other hand, for cases where the initial state is stable, the parameter optimization also plays a role.

It is not difficult to infer a preliminary conclusion that a larger power generation capacity and longer electrical distance will cause more drastic stability changes to MGCCSs

due to the fine-tuning of inverter control parameters.

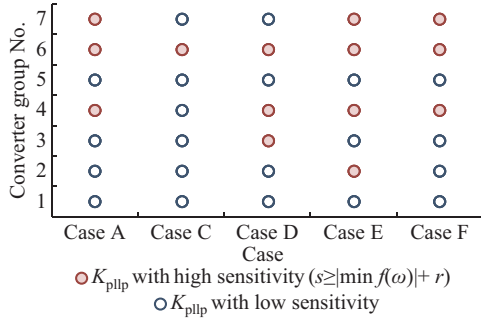


Fig. 10. Screening high-sensitivity parameters in different cases.

Meanwhile, Fig. 11 shows the solving processes of $\min f(\omega)$ with different control parameters in Case A. Their difference lies in different input variables. Theoretically, better results can be obtained when the variables of high-sensitivity parameters are input.

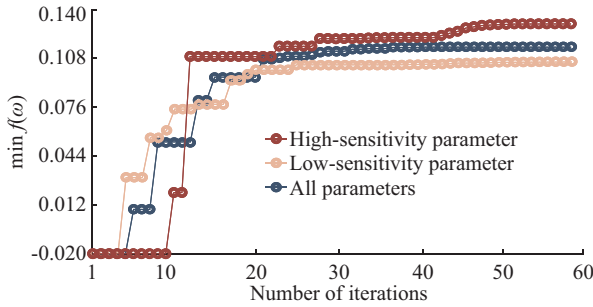


Fig. 11. Solving processes of $\min f(\omega)$ with different control parameters in Case A.

After the input variables of optimization algorithm are identified, this paper uses four algorithms to solve the optimization model, as shown in Fig. 12. The control parameter settings for PSO, SA, GA, and DEA can be found in Tables IV-VII, respectively, where the maximum iterations and swarm sizes are all 60 and 20.

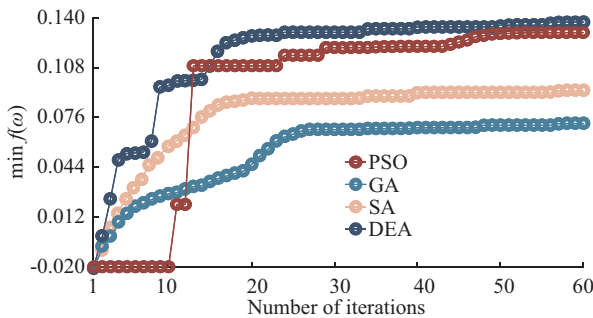


Fig. 12. Solving processes of $\min f(\omega)$ with different algorithms in Case A.

TABLE IV
PARAMETER SETTING FOR PSO

Parameter	Description	Value
c_1	Range of personal learning coefficient	0.5-2.5
c_2	Range of global learning coefficient	0.5-2.5
w	Range of inertia weight	0.4-0.9

TABLE V
PARAMETER SETTINGS FOR SA

Parameter	Description	Value
T_0	Initial temperature	200
C_s	Cooling rate	0.95
T_{\min}	Final temperature	0.01

TABLE VI
PARAMETER SETTINGS FOR GA

Parameter	Description	Value
P_c	Crossover probability	0.75
P_m	Mutation probability	0.05

TABLE VII
PARAMETER SETTINGS FOR DEA

Parameter	Description	Value
F	Scale factor	1.0
P_c	Crossover probability	0.7

It is worth mentioning here that the value of $\min f(\omega)$ is low at the beginning of iteration. This is because the optimization algorithm will seek optima in a certain neighborhood of the current operating parameters. And in this neighborhood, the correction trend of the control parameters cannot be guaranteed to be consistent with that of the sensitivity function. As the number of iterations increases, the optimization algorithm will learn this trend and eventually converge.

The simulation model is established based on the electromagnetic transient simulation software PSCAD/EMTDC. With this test model, extensive simulations can be performed to verify the effectiveness of the proposed adaptive control strategy.

Figure 13 illustrates the transient response waveforms of the active power when the MGCCSs operate with control parameters optimized by the DEA, PSO, SA, and GA, following the disturbance applied at $t=0.4$ s.

Specifically, DEA exhibits the optimal performance, characterized by the minimum initial power drop, negligible subsequent oscillations, and the fastest recovery, demonstrating superior disturbance rejection capability. In contrast, PSO shows a more pronounced initial drop and oscillation compared with DEA. SA, despite an initial drop, experiences more severe and prolonged oscillations compared with PSO. GA performs the worst, exhibiting not only the largest initial drop but also the most severe and persistent subsequent power oscillations, resulting in the slowest recovery.

Considering the initial deviation, oscillation magnitude, and recovery time, the disturbance rejection performance with these algorithms is clearly ranked as: DEA comes first, followed by PSO, then SA, and GA is the last. However, the stable optimization model requires a high computational speed. Although DEA performs the best in terms of convergence, it consumes too much time. Therefore, in the subsequent analysis, this paper takes the PSO with the fastest computational speed as an example.

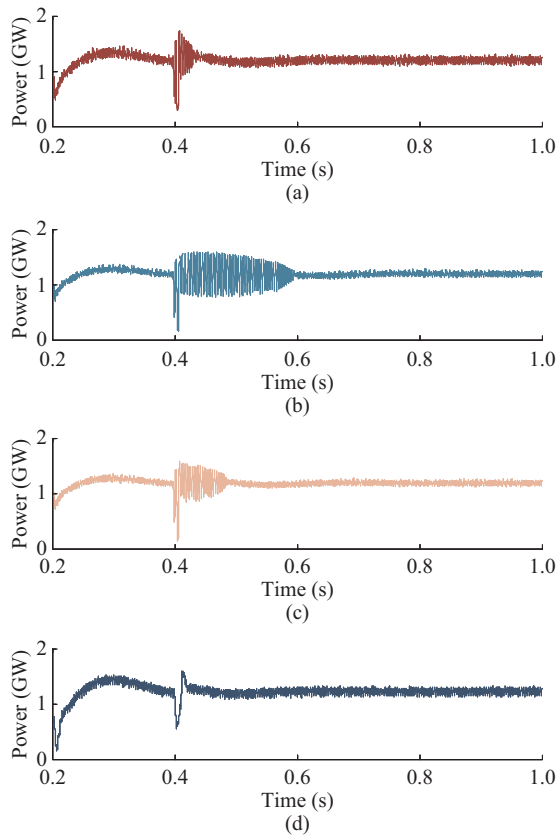


Fig. 13. Transient response waveforms of active power when MGCCSs operate with control parameters optimized by PSO, GA, SA, and DEA. (a) PSO. (b) GA. (c) SA. (d) DEA.

To better demonstrate the adaptability of PSO under different operating conditions, this paper simulates the power grid intensity changes within 24 hours of a day with a sampling interval of 15 min. From Fig. 14, when the operating state enters the region with instability risk, the PSO adjusts the control parameters of inverters. This helps escape the risk of instability and operate with a higher small-signal stability margin.

According to the previous analysis, in Case A, the value of $\min f(\omega)$ describing the small-signal stability of MGCCSs is -0.02 , and the system is considered exhibiting oscillatory divergence. In Case B, the MGCCSs are considered stable due to $\min f(\omega)=0.132$. When the system operates in Case A and Case B, the three-phase voltages at PCC are shown in Fig. 15(a) and (b), respectively, where converters are connected to power grid at $t=0.5$ s. At this point, based on the above analysis results, it can be known that the voltage does indeed oscillate and diverge as expected in Case A, and operates stably in Case B.

Meanwhile, the system output power is shown in Fig. 16. In Case B, after interference injection, the system returns to normal operation after a brief fluctuation. The small-signal stability margin of the system in Case B is higher than that in Case A. Therefore, the effectiveness of the proposed adaptive control strategy in improving the small-signal stability has been experimentally verified.

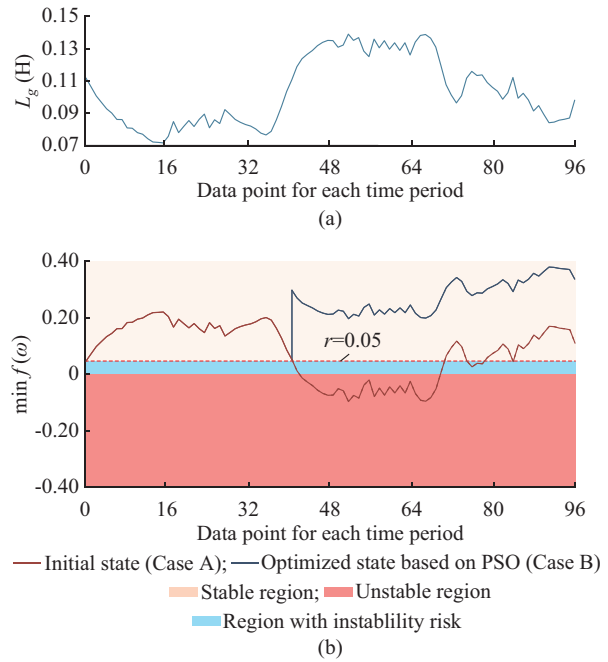


Fig. 14. Stability improvement of MGCCSs based on PSO algorithm. (a) Variation of impedance L_g of power grid. (b) $\min f(\omega)$.

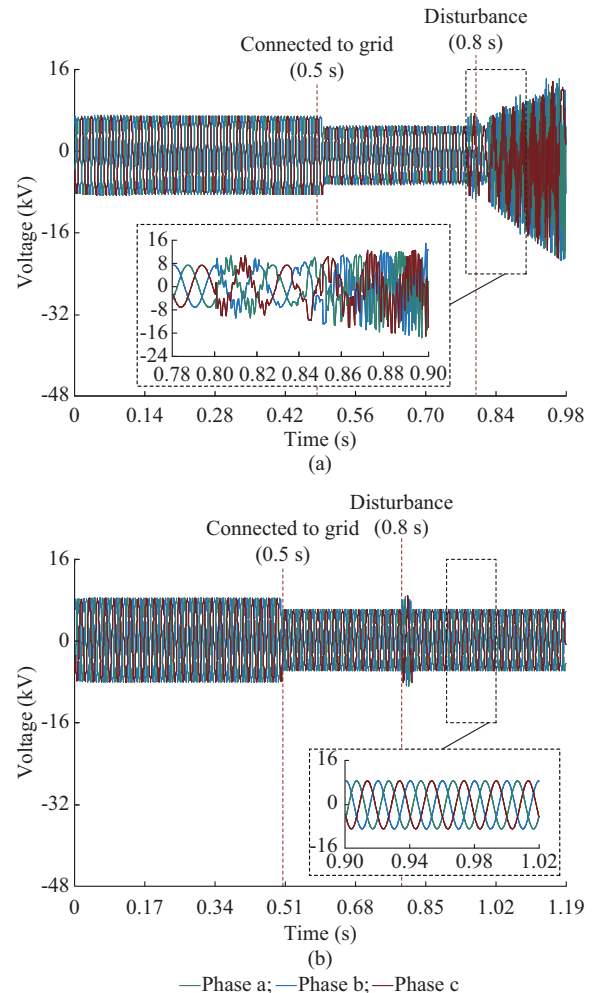


Fig. 15. Three-phase voltage at PCC in Case A and Case B. (a) Case A. (b) Case B.

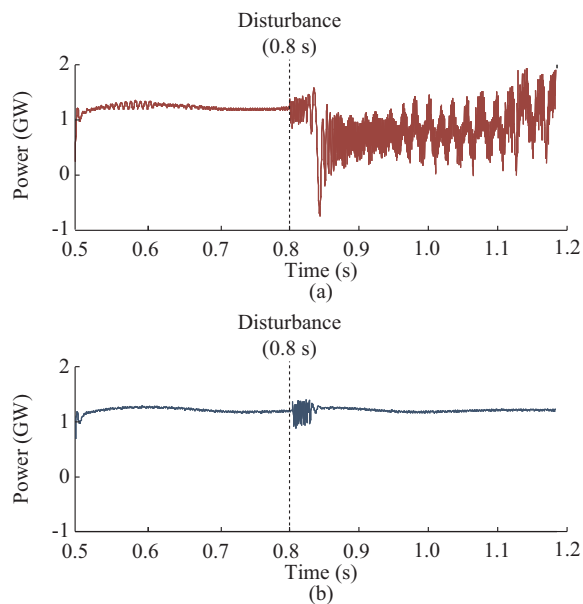


Fig. 16. System output power in Case A and Case B. (a) Case A. (b) Case B.

V. CONCLUSION

The main contributions and significance of this paper are summarized as follows.

1) This paper proposes the sensitivity criterion of the control parameters of MGCCSs. In the process of solving the control parameters by using the optimization algorithm, the input variables can be screened according to the parameter sensitivities to ensure a high convergence speed and calculation speed. In the power system with large-scale renewable energy, the proposed adaptive control strategy provides a new way to eliminate the adverse effect of the high-dimensional characteristic of impedance ratio matrix on the optimization algorithm.

2) The proposed adaptive control strategy can clarify the influence of control parameters on the small-signal stability of MGCCSs, and provide guidance for the design of control parameters. Meanwhile, when facing the characteristics of random and volatile output of renewable energy, the proposed adaptive control strategy still can compensate for system small-signal stability margin online.

REFERENCES

- [1] X. Wang and F. Blaabjerg, "Harmonic stability in power electronic-based power systems: concept, modeling, and analysis," *IEEE Transactions on Smart Grid*, vol. 10, no. 3, pp. 2858-2870, May 2019.
- [2] C. Wang, W. Zheng, Z. Wang *et al.*, "Partition-based network equivalent method for power system subsynchronous oscillation analysis," *Journal of Modern Power Systems and Clean Energy*, vol. 12, no. 1, pp. 313-320, Jan. 2024.
- [3] Y. Chen, H. Tian, G. Zheng *et al.*, "Operation strategy of rail transit green energy system considering uncertainty risk of photovoltaic power output," *Journal of Modern Power Systems and Clean Energy*, vol. 12, no. 6, pp. 1859-1868, Nov. 2024.
- [4] S. Kamala, N. B. Y. Gorla, and S. K. Panda, "Small-signal stability improvement of microgrid with battery energy storage system based on real-time grid impedance measurement," *IEEE Transactions on Industry Applications*, vol. 58, no. 2, pp. 2537-2546, Jan. 2022.
- [5] J. Kwon, X. Wang, C. L. Bak *et al.*, "The modeling and harmonic coupling analysis of multiple-parallel connected inverter using harmonic state space (HSS)," in *Proceedings of 2015 IEEE Energy Conversion Congress and Exposition*, Montreal, Canada, Sept. 2015, pp. 6231-6238.
- [6] Q. Chen, S. Bu, and C. Y. Chung, "Small-signal stability criteria in power electronics-dominated power systems: a comparative review," *Journal of Modern Power Systems and Clean Energy*, vol. 12, no. 4, pp. 1003-1018, Dec. 2023.
- [7] M. Esparza, J. Segundo-Ramirez, J. B. Kwon *et al.*, "Modeling of VSC-based power systems in the extended harmonic domain," *IEEE Transactions on Power Electronics*, vol. 32, no. 8, pp. 5907-5916, Aug. 2017.
- [8] R. Pan, G. Tang, S. Liu *et al.*, "Impedance analysis of grid forming control based modular multilevel converters," *Journal of Modern Power Systems and Clean Energy*, vol. 11, no. 3, pp. 967-979, May 2023.
- [9] Y. Ren, X. Wang, L. Chen *et al.*, "A strictly sufficient stability criterion for grid-connected converters based on impedance models and Gershgorin's theorem," *IEEE Transactions on Power Delivery*, vol. 35, no. 3, pp. 1606-1609, Jun. 2020.
- [10] Z. Liu, Y. Chen, Z. Zhang *et al.*, "Identification of vulnerable nodes and sensitivity analysis of control parameters for multiple grid-connected converter systems," *IEEE Transactions on Sustainable Energy*, vol. 16, no. 3, pp. 1602-1612, Dec. 2024.
- [11] A. Argüello, "Setpoint feasibility and stability of wind park control interactions at weak grids," *Journal of Modern Power Systems and Clean Energy*, vol. 10, no. 6, pp. 1790-1796, Jun. 2022.
- [12] E. Ebrahimzadeh, F. Blaabjerg, X. Wang *et al.*, "Harmonic stability and resonance analysis in large PMSG-based wind power plants," *IEEE Transactions on Sustainable Energy*, vol. 9, no. 1, pp. 12-23, Jan. 2018.
- [13] T. Lin, R. Chen, G. Yu *et al.*, "Extended gershgorin theorem-based parameter feasible domain to prevent harmonic resonance in power grid," *Energies*, vol. 10, no. 10, p. 1612, Oct. 2017.
- [14] Y. Zhan, X. Xie, H. Liu *et al.*, "Frequency-domain modal analysis of the oscillatory stability of power systems with high-penetration renewables," *IEEE Transactions on Sustainable Energy*, vol. 10, no. 3, pp. 1534-1543, Jul. 2019.
- [15] J. Pedra, L. Sainz, and L. Monjo, "Three-port small signal admittance-based model of VSCs for studies of multi-terminal HVDC hybrid AC/DC transmission grids," *IEEE Transactions on Power Systems*, vol. 36, no. 1, pp. 732-743, Jun. 2020.
- [16] Y. Li, Z. Shuai, X. Liu *et al.*, "Stability analysis and location optimization method for multiconverter power systems based on nodal admittance matrix," *IEEE Journal of Emerging and Selected Topics in Power Electronics*, vol. 9, no. 1, pp. 529-538, Feb. 2021.
- [17] Y. Ren, R. Duan, L. Chen *et al.*, "Stability assessment of grid-connected converter system based on impedance model and Gershgorin theorem," *IEEE Transactions on Energy Conversion*, vol. 35, no. 3, pp. 1559-1566, Sept. 2020.
- [18] Z. Liu, J. Zhao, K. Qu *et al.*, "A small-signal stability criterion for DC microgrid based on extended-Gershgorin theorem," *IEEE Transactions on Power Delivery*, vol. 38, no. 3, pp. 2047-2057, Jan. 2023.
- [19] Z. Zeng, J. Zhao, Z. Liu *et al.*, "Stability assessment for multiple grid-connected converters based on impedance-ratio matrix and Gershgorin's Theorem," *International Journal of Electrical Power & Energy Systems*, vol. 138, p. 107869, Jun. 2022.
- [20] L. Wang, X. Xie, Q. Jiang *et al.*, "Investigation of SSR in practical DFIG-based wind farms connected to a series-compensated power system," *IEEE Transactions on Power Systems*, vol. 30, no. 5, pp. 2772-2779, Sept. 2015.
- [21] M. V. Gururaj and N. P. Padhy, "A cost-effective single architecture to operate DC microgrid interfaced DFIG wind system during grid-connected, fault, and isolated conditions," *IEEE Transactions on Industrial Informatics*, vol. 16, no. 2, pp. 922-934, Feb. 2020.
- [22] L. Huang, H. Xin, Z. Li *et al.*, "Grid-synchronization stability analysis and loop shaping for PLL-based power converters with different reactive power control," *IEEE Transactions on Smart Grid*, vol. 11, no. 1, pp. 501-516, Jun. 2019.
- [23] Z. Zeng, H. Xiao, C. Niu *et al.*, "An improved impedance modeling method of grid-tied inverters with white-box property," *IEEE Transactions on Power Electronics*, vol. 37, no. 4, pp. 3980-3989, Oct. 2021.
- [24] X. Wang, L. Harnefors, and F. Blaabjerg, "Unified impedance model of grid-connected voltage-source converters," *IEEE Transactions on Power Electronics*, vol. 33, no. 2, pp. 1775-1787, Feb. 2018.
- [25] C. Yang, L. Huang, H. Xin *et al.*, "Placing grid-forming converters to enhance small signal stability of PLL-integrated power systems," *IEEE Transactions on Power Systems*, vol. 36, no. 4, pp. 3563-3573, Jul. 2021.
- [26] C. H. Liu and Y. Y. Hsu, "Design of a self-tuning PI controller for a

STATCOM using particle swarm optimization,” *IEEE Transactions on Industrial Electronics*, vol. 57, no. 2, pp. 702-715, Feb. 2010.

- [27] H. Shutari, N. Saad, N. B. M. Nor *et al.*, “Towards enhancing the performance of grid-tied VSMT via adopting sine cosine algorithm-based optimal control scheme,” *IEEE Access*, vol. 9, pp. 139074-139088, Oct. 2021.
- [28] M. A. Memon, M. D. Siddique, S. Mekhilef *et al.*, “Asynchronous particle swarm optimization-genetic algorithm (APSO-GA) based selective harmonic elimination in a cascaded H-bridge multilevel inverter,” *IEEE Transactions on Industrial Electronics*, vol. 69, no. 2, pp. 1477-1487, Feb. 2021.
- [29] A. H. Roger, *Matrix Analysis*. Cambridge: Cambridge University Press, 1985.

Zhenxiang Liu received the B.Eng. and M.Eng. degrees from Shanghai University of Electric Power, Shanghai, China, in 2020 and 2023, respectively. He is currently working toward the Ph.D. degree in electrical engineering with North China Electric Power University, Beijing, China. His research interests include AC/DC system stability analysis and control of smart grid.

Yanbo Chen received the B.S. degree in electrical engineering from Huazhong University of Science and Technology, Wuhan, China, in 2007, the M. S. degree in electrical engineering from China Electric Power Research Institute, Beijing, China, in 2010, and the Ph.D. degree in electrical engineering from Tsinghua University, Beijing, China, in 2013. He is currently a Professor with North China Electric Power University, Beijing, China. His research interests include state estimation and power system analysis and control.

Jiahao Ma received the B.Eng. degree from Harbin Institute of Technology, Harbin, China, in 2022. He is currently working toward the master’s degree in electrical engineering with North China Electric Power University, Beijing, China. His research interests include stability analysis and control technology for new energy grid-connected and grid-following converter.

Zhi Zhang received the B.S. degree in electrical engineering from China Three Gorges University, Yichang, China, in 2017, and the M.S. and Ph.D. degrees in electrical engineering from North China Electric Power University, Beijing, China, in 2020 and 2023, respectively. Since 2023, he has been with the School of Electrical and Electronic Engineering, North China Electricity Power University, where he is currently an Assistant Professor. His research interests include power system operation and control.